

OPTIMAL PATH PLANNING FOR A DYNAMIC PLATFORM

Horn-Yong Jan,¹ Chun-Liang Lin,² and Jr-Rong Lin³

1. Graduate Institute of Electrical and Communications Engineering,
Feng Chia University,
Taichung, Taiwan 40724, R.O.C.

Email: p9112206@knight.fcu.edu.tw

2. Department of Electrical Engineering
National Chung Hsing University
Taichung 402, Taiwan, R.O.C.

3. Institute of Automatic Control Engineering
Feng Chia University
Taichung 40724, Taiwan, R.O.C.

Abstract: This paper presents a complete modelling, singularity characterization and path planning design for a newly developed 3 legs 6 degree-of-freedom (DOFs) parallel manipulator. In the presented architecture, the base platform has three linear slideways actuated respectively by a linear DC motor, and each extensible vertical link connecting the upper and base platforms is actuated by an inductive AC servo motor. Special emphasis is put on characterizing the platform singularity characterization and singularity avoidance of the moving platform path planning based on DNA algorithms. A new path planning scheme is proposed which uses a DNA search algorithm, whose coding technique speeds up the execution of DNA search, for fast path generation on the available workspace. *Copyright © 2005 IFAC*

Keywords: linear motors, kinematics, genetic algorithms, path planning.

1. INTRODUCTION

The Stewart platform is an example of a parallel connection robot manipulator which was obtained from generalization of the mechanism originally proposed by Stewart (Stewart, 1965). Each leg is connected to the base by a two degree-of-freedom (DOF) universal joint and connected to the moving platform by 3-DOF spherical joints (Fichter, 1986).

There has been many research topics concerning Stewart platforms were presented which included platform construction, singularity and working space determination, forward and inverse kinematic solutions, dynamic forces computation, motion control, and practical applications (Raghavan, 1993; Ceccarelli, 1997; Wang, *et al.*, 1997, Ryu, *et al.*, 2001; Honegger, *et al.*, 1997). Recently, great interests in the design of spatial multiple-DOF parallel manipulators for specific purposes were extensively developed (Ceccarelli, 1997; Wang, *et al.*, 1997, Ryu, *et al.*, 2001).

In this paper, we present the modeling and analysis of a new 6-DOF platform manipulator which has three linear slideways, each actuated by a linear DC

motor, where each flexible vertical link connecting the upper and base platforms is actuated by an inductive AC servo motor.

Genetic algorithms (GAs) and evolutionary algorithms (EAs) have been widely applied for system optimization and industrial applications in recent years. GAs and EAs, DNA computing methods, pioneered by Adleman (1998) who showed the potential of using bio-molecules for effectively solving computational problems, have recently captured more and more attention (Garzon, *et al.*, 1999) since DNA sequences encode plentiful genetic information. Advantages of DNA computing are massive parallelism and enormous information storage capability. These benefits allow a large problem space that can be reached in almost limited time. In (Kiguchi, *et al.*, 2001), the planar trajectory planning of mobile robots was addressed using Watson-Crick pairing. In (Ding, *et al.*, 2000), the authors proposed a DNA genetic method to design the generalized membership-type Takagi-Sugeno fuzzy control system and applied it to robot motion control.

In the proposed approach, the search space is divided into several slices in which less blocks of every slices

correspond to the areas containing loosely dense singularities and vice versa. The shortest path for singularities avoidance in the search space is characterized with the DNA evolutionary process. The proposed approach is verified by checking a variety of scenarios of the path planning problem.

2. PLATFORM KINEMATICS

2.1 Coordinates transformation

The parallel manipulator under consideration consists of a lower base platform, an upper platform, three flexible vertical links, and three actuating horizontal links. Each horizontal link is actuated by a synchronous linear motor, and each flexible vertical link is actuated by an inductive AC servo motor, see Fig. 1. Figure 2 shows the top view of the upper (moving) and base platforms. In Fig. 2, ${}^P\mathbf{P}_i$ ($i=1,2,3$) denote the position vectors of the joint points between the three links and the moving platform, which are concentric joint points with respect to the upper platform coordinate frame $\{P\}$, \mathbf{B}_i ($i=1,2,3$) denote the position vectors of the joint points on the base platform with respect to the base platform coordinate frame $\{B\}$.

We denote the Cartesian coordinate vector $\mathbf{X}=[\mathbf{p} \ \boldsymbol{\vartheta}]^T$, where $\mathbf{p}=[x \ y \ z]^T$ and $\boldsymbol{\vartheta}=[\phi \ \theta \ \psi]^T$ denotes the position and orientation of the moving platform's mass center respectively, the joint coordinate vector $\mathbf{q}=[l_1 \ l_2 \ l_3 \ d_1 \ d_2 \ d_3]^T$,

where l_i is the length of the i -th vertical link, and d_i is the distance between the i th joint and the starting position of the slide way on the base platform.

The coordinate transformation from the coordinate system $\{P\}$ with respect to the inertial coordinate system $\{B\}$ is given by

$$\mathbf{R} = \begin{bmatrix} c\psi c\theta & c\psi s\theta s\phi - s\psi c\phi & c\psi s\theta c\phi + s\psi s\phi \\ s\psi c\theta & s\psi s\theta s\phi + c\psi c\phi & s\psi s\theta c\phi - c\psi s\phi \\ -s\theta & c\theta s\phi & c\theta c\phi \end{bmatrix} \quad (1)$$

2.2 Inverse Kinematics

For the base platform, the coordinates of the hexagon terminal points shown in Fig. 2 are

$$\begin{aligned} \mathbf{BB}_1 &= \left(-\frac{2}{3}B, k, 0\right), & \mathbf{BB}_2 &= \left(\frac{B}{3} - k_1, \frac{2}{3}B \cos \frac{\pi}{6} + k_2, 0\right) \\ \mathbf{BB}_3 &= \left(\frac{B}{3} - k_1, \frac{2}{3}B \cos \frac{\pi}{6} - k_2, 0\right), & \mathbf{BB}_4 &= \left(\frac{B}{3} + k_1, -\frac{2}{3}B \cos \frac{\pi}{6} + k_2, 0\right) \\ \mathbf{BB}_5 &= \left(\frac{B}{3} - k_1, -\frac{2}{3}B \cos \frac{\pi}{6} - k_2, 0\right) & \mathbf{BB}_6 &= \left(-\frac{2}{3}B, k, 0\right) \end{aligned}$$

where B is the height of the equilateral triangular forming within the base plate, k is the half length from \mathbf{BB}_1 to \mathbf{BB}_6 with $k_1 = k \sin \frac{\pi}{6}$ and $k_2 = k \cos \frac{\pi}{6}$.

For simplicity, this can be represented in a compact form:

$$\mathbf{L}_i = \mathbf{T}_v + \mathbf{R}^P \mathbf{P}_i - \mathbf{B}_i, i=1,2,3 \quad (2)$$

where \mathbf{T}_v denotes the origin's line vector of frame $\{P\}$ with respect to frame $\{B\}$. Considering the relative position between the joint of the upper platform and linear motor's translator on the base platform illustrated

$$B_{iy} = \frac{B_{biy} - B_{aiy}}{B_{bix} - B_{aix}} B_{ix} + \frac{B_{bix} B_{aiy} - B_{biy} B_{aix}}{B_{bix} - B_{aix}}, \quad i=1,2,3 \quad (3)$$

where $\mathbf{B}_{ai} = [B_{aix} \ B_{aiy} \ 0]^T$ and $\mathbf{B}_{bi} = [B_{bix} \ B_{biy} \ 0]^T$ and we have the following constraints:

$$(\mathbf{B}_{bi} - \mathbf{B}_{ai}) \mathbf{L}_i = 0, i=1,2,3 \quad (4)$$

Combining (3) and (4) B_{ix} can be solved for the motors' translators as

$$B_{ix} = \frac{(B_{bix} - B_{aix}) P_{ix} + (P_{iy} - C)(B_{biy} - B_{aiy})}{B_{bix} - B_{aix} + A(B_{biy} - B_{aiy})} \quad (5)$$

where

$$A = \frac{B_{biy} - B_{aiy}}{B_{bix} - B_{aix}}, \quad C = \frac{B_{bix} B_{aiy} - B_{biy} B_{aix}}{B_{bix} - B_{aix}}$$

In summary, constraint equations of the links are characterized by

$$\Phi_{i1} = (\mathbf{P}_i - \mathbf{B}_i)^T (\mathbf{P}_i - \mathbf{B}_i) - l_i^2 = 0, i=1,2,3 \quad (6)$$

$$\Phi_{i2} = (\mathbf{P}_i - \mathbf{B}_i)^T \mathbf{d}_k = 0, i=4,5,6, \quad k=i-3 \quad (7)$$

where \mathbf{d}_k is the unit vector of the linear motor's slide way.

Next, attention is turned to the link frames $\{i, j, k\}$ $i=1,2,3$. The unit vectors of the link coordinate iXYZ are defined as

$$\mathbf{i}_i = \frac{\mathbf{L}_i}{\|\mathbf{L}_i\|} = i_{ix} \mathbf{i} + i_{iy} \mathbf{j} + i_{iz} \mathbf{k} \quad (8)$$

$$\mathbf{j}_i = \frac{\mathbf{i}_i \times (-\mathbf{k})}{\|\mathbf{i}_i \times (-\mathbf{k})\|} = i_{ix} \mathbf{i} + i_{iy} \mathbf{j} + i_{iz} \mathbf{k} \quad (9)$$

$$\mathbf{k}_i = \mathbf{i}_i \times \mathbf{j}_i = k_{ix} \mathbf{i} + k_{iy} \mathbf{j} + k_{iz} \mathbf{k} \quad (10)$$

The coordinate transformation matrix from frame $\{B\}$ to frame $\{i\}$ is the transpose of \mathbf{R}_i :

$$\mathbf{R}_i = \mathbf{R}_i^T = \begin{bmatrix} i_{ix} & i_{iy} & i_{iz} \\ j_{ix} & j_{iy} & j_{iz} \\ k_{ix} & k_{iy} & k_{iz} \end{bmatrix}, i=1,2,3 \quad (11)$$

We first rotate frame $\{B\}$ about Z -axis by an angle ϕ_i to get frame $\{B'\}$, then rotate $\{B'\}$ about Y' -axis by an angle θ_i to get frame $\{B''\}$ and finally rotate $\{B''\}$ about Z'' -axis by an angle ψ_i to get frame $\{i\}$. The sequence gives a transformation matrix as follows

$$\mathbf{R}_i = \mathbf{R}_{Z,\phi_i} \mathbf{R}_{Y',\theta_i} \mathbf{R}_{Z'',\psi_i} = \begin{bmatrix} c\phi_i c\theta_i c\psi_i - s\phi_i s\psi_i & -c\phi_i c\theta_i s\psi_i - s\phi_i c\psi_i & c\phi_i s\theta_i \\ s\phi_i c\theta_i c\psi_i + c\phi_i s\psi_i & -s\phi_i c\theta_i s\psi_i + c\phi_i c\psi_i & s\phi_i s\theta_i \\ -s\theta_i c\psi_i & s\theta_i s\psi_i & c\theta_i \end{bmatrix} \quad (12)$$

Combining (11) and (12), the corresponding Euler angles of the i th link can be obtained as

$$\begin{aligned}\phi_i &= \tan^{-1}\left(\frac{k_{iy}}{k_{ix}}\right) \\ \theta_i &= \tan^{-1}\left(\frac{k_{ix} \cos \phi_i + k_{iy} \sin \phi_i}{k_{iz}}\right) \\ \psi_i &= \tan^{-1}\left(\frac{-i_{ix} \sin \phi_i + i_{iy} \cos \phi_i}{-j_{ix} \sin \phi_i + j_{iy} \cos \phi_i}\right)\end{aligned}\quad (13)$$

Since the vertical link is orthogonal to the horizontal link for this specific architecture, the angle ϕ_i can be determined for the given slideways. Also, all ψ_i are zeros. The angular velocity $\boldsymbol{\omega}_i$ expressed by Euler angles can then be represented with respect to link frame $\{i\}$ as

$$\boldsymbol{\omega}_i = \dot{\phi}_i \mathbf{k} + \dot{\theta}_i \mathbf{j}' + \dot{\psi}_i \mathbf{k}'' = \begin{bmatrix} -\dot{\phi}_i c\psi_i s\theta_i + \dot{\theta}_i s\psi_i \\ \dot{\phi}_i s\psi_i s\theta + \dot{\theta}_i c\psi_i \\ \dot{\phi}_i c\theta_i + \dot{\psi}_i \end{bmatrix} \quad (14)$$

The angular acceleration $\boldsymbol{\alpha}_i$ of the i th link can also be obtained as

$$\boldsymbol{\alpha}_i = \begin{bmatrix} -\ddot{\phi}_i c\psi_i s\theta_i + \dot{\phi}_i (\dot{\psi}_i s\psi_i s\theta_i - \dot{\theta}_i c\psi_i c\theta_i) + \ddot{\theta}_i s\psi_i + \dot{\theta}_i \dot{\psi}_i c\psi_i \\ \ddot{\phi}_i s\psi_i s\theta + \dot{\phi}_i (\dot{\psi}_i c\psi_i s\theta_i + \dot{\theta}_i s\psi_i c\theta_i) + \ddot{\theta}_i c\psi_i - \dot{\theta}_i \dot{\psi}_i s\psi_i \\ \ddot{\phi}_i c\theta_i - \dot{\phi}_i \dot{\theta}_i s\theta_i + \ddot{\psi}_i \end{bmatrix} \quad (15)$$

Similarly, the angular velocity $\boldsymbol{\omega}_p$ can be represented as

$$\boldsymbol{\omega}_p = \dot{\psi}_p \mathbf{k} + \dot{\theta}_p \mathbf{j}' + \dot{\phi}_p \mathbf{k}'' = \begin{bmatrix} -\dot{\psi}_p s\theta_p + \dot{\phi}_p \\ \dot{\psi}_p c\theta_p s\phi_p + \dot{\theta}_p c\phi_p \\ \dot{\psi}_p c\theta_p c\phi_p - \dot{\theta}_p s\phi_p \end{bmatrix} \quad (16)$$

The angular acceleration $\boldsymbol{\alpha}_p$ can be obtained straightforward as

$$\boldsymbol{\alpha}_p = \begin{bmatrix} -\ddot{\psi}_p s\theta_p - \dot{\psi}_p \dot{\theta}_p c\theta_p + \ddot{\phi}_p \\ \ddot{\psi}_p c\theta_p s\phi_p - \dot{\psi}_p (\dot{\theta}_p s\theta_p s\phi_p - \dot{\phi}_p c\theta_p c\phi_p) + \ddot{\theta}_p c\phi_p - \dot{\theta}_p \dot{\phi}_p s\phi_p \\ \ddot{\psi}_p c\theta_p c\phi_p - \dot{\psi}_p (\dot{\theta}_p s\theta_p c\phi_p + \dot{\phi}_p c\theta_p s\phi_p) - \ddot{\theta}_p s\phi_p - \dot{\theta}_p \dot{\phi}_p c\phi_p \end{bmatrix} \quad (17)$$

3. DYNAMICS ANALYSIS

3.1 Link Dynamics

Let us first focus on the i th link's mass center O_i . Each link is placed along the X_i axis; therefore, its inertia tensor about X_i , Y_i and Z_i is a diagonal matrix with diagonal elements I_{ixx} , I_{iyy} and I_{izz} . The angular momentum of the i th link is

$$\mathbf{H}_i = I_{ixx} \boldsymbol{\omega}_i \mathbf{i}_i + I_{iyy} \boldsymbol{\omega}_i \mathbf{j}_i + I_{izz} \boldsymbol{\omega}_i \mathbf{k}_i \quad (18)$$

$$\dot{\mathbf{H}}_i = (\dot{\mathbf{H}}_i)_{xyz} + \boldsymbol{\omega}_i \times \mathbf{H}_i \quad (19)$$

It follows from Fig. 3 that the torque about the link's mass center O_i is given by

$$\sum \mathbf{M}_{O_i} = {}^i \mathbf{r}_{pi} \times {}^i \mathbf{F}_{pi} + {}^i \mathbf{r}_{bi} \times {}^i \mathbf{F}_{bi} \quad (20)$$

where ${}^i \mathbf{r}_{pi}$ is the vector from O_i to P_i with respect to the link frame $\{i\}$ and ${}^i \mathbf{r}_{bi}$ is the vector from O_i to B_i with respect to frame $\{i\}$.

We now proceed to find the total force acting on the link's mass center. It can be seen from the free-body diagram of Fig. 3 that

$${}^i \mathbf{F}_{bi} - {}^i \mathbf{F}_{pi} - \mathbf{R}_i^T \mathbf{W}_{li} = m_{li} {}^i \ddot{\mathbf{r}}_{ic.m} \quad (21)$$

where $\mathbf{W}_{li} = [0 \ 0 \ W_{liz}]^T$, with W_{liz} and m_{li} being, respectively, the weight and mass of the i th link; and the acceleration at the link's mass center is given by

$$\begin{aligned}{}^i \ddot{\mathbf{r}}_{ic.m} &= \mathbf{R}_i^T \ddot{\mathbf{r}}_{Bi} + {}^i \ddot{\mathbf{r}}_{Bic} = \mathbf{R}_i^T \ddot{\mathbf{r}}_{Bi} + \boldsymbol{\alpha}_i \times {}^i \mathbf{r}_{Bic} + \boldsymbol{\omega}_i \times (\boldsymbol{\omega}_i \times {}^i \mathbf{r}_{Bic}) \\ {}^i F_{piz} &= [I_{izx} W_{iz} W_{ix} - I_{ixx} W_{ix} W_{iz} - I_{iyy} \dot{W}_{iy} - {}^i r_{ix} m_i \dot{r}_{ic.mc} - {}^i r_{bix} (c\theta_i) W_{liz}] / ({}^i r_{pix} + {}^i r_{bix})\end{aligned}\quad (22)$$

where ${}^i r_{pix}$ and ${}^i r_{bix}$ have the same length as ${}^i r_{Bicx}$. Substituting ${}^i F_{piz}$ from (22), we can get ${}^i F_{biz}$.

3.2 Moving Platform Dynamics

Only the force terms ${}^i F_{piz}$ and ${}^i F_{biz}$ were obtained in the equations of link motion, so to calculate the force terms ${}^i F_{pix}$ and ${}^i F_{piy}$ the moving platform dynamics should be taken into consideration.

The angular momentum of the moving platform is described by

$$\mathbf{H}_p = I_{pax} \boldsymbol{\omega}_p \mathbf{i}_p + I_{pby} \boldsymbol{\omega}_p \mathbf{j}_p + I_{paz} \boldsymbol{\omega}_p \mathbf{k}_p \quad (23)$$

where I_{pax} , I_{pby} and I_{paz} are the mass moments of inertia of the upper platform about X, Y and Z axes of frame $\{P\}$ respectively. The corresponding angular momentum change is

$$\dot{\mathbf{H}}_p = (\dot{\mathbf{H}}_p)_{xyzp} + \boldsymbol{\omega}_p \times \mathbf{H}_p \quad (24)$$

The total torque acting on the moving platform mass center O_p is given by

$$\sum \mathbf{M}_{O_p} = \sum_{i=1}^3 {}^p \mathbf{P}_i \times {}^p \mathbf{F}_{pi} \quad (25)$$

where ${}^p \mathbf{F}_{pi} = \mathbf{R}^T \mathbf{R}_i {}^i \mathbf{F}_{pi} = \mathbf{R}_{pi} {}^i \mathbf{F}_{pi}$, ${}^p \mathbf{F}_{pi}$ can be expressed in coordinate frame $\{i\}$ by the rotation matrix $\mathbf{R}_{pi} = \mathbf{R}^T \mathbf{R}_i$. From Fig. 5 we have the force equation acting on O_p :

$$-\mathbf{W}_p + \sum_{i=1}^3 \mathbf{R}_i + {}^i \mathbf{F}_{pi} = m_p \mathbf{a}_p \quad (26)$$

where $\mathbf{W}_p = [0 \ 0 \ W_p]^T$, with W_p and m_p being, respectively, the weight and mass of the moving platform; and \mathbf{a}_p denotes the acceleration of the moving platform. Furthermore, the actuating force on each vertical link can be calculated as follows

$${}^i \mathbf{F}_{iact} = {}^i F_{pix} + \mathbf{R}_i^T \mathbf{W}_{li} + m_{li} {}^i \ddot{\mathbf{r}}_{bic}'' \quad (27)$$

4. EXPERIMENTAL ARCHITECTURE

Optimal mechanism of the platform is designed by means of the Taguchi Method (Madhav, 1989) to maximize orientation of the moving platform under the constraint of the slide range of the translators of

linear motors. With the prespecified slide range $S_i = 270$ mm and length of the link $l_i = 300$ mm, the experimental results give the radius of the moving platform $R_p = 230$ mm, the radius of the base platform $R_b = 1050$ mm, the height of the upper platform $Z_h = 550$ mm.

5. SINGULARITY ANALYSIS BASED ON GA

The configuration singularity depends only on individual configuration. Based on the inverse kinematic equation, the angle change of the moving platform orientation can be tested when $z=1050$ mm. The maximal orientation angles of the presented platform are given by $\phi = 124$ deg, $\theta = 164$ deg, and $\psi = 74$ deg.

To proceed, we first determine the Jacobian matrix and then propose a genetic searching algorithm to find singular points. Differentiating (6) and (7) with respect to time t gives

$$\frac{\partial \Phi_{ij}}{\partial t} = \Phi_x \dot{X} + \Phi_q \dot{q} = 0, i=1, \dots, 6, j=1, 2 \quad (28)$$

i.e.

$$J\dot{X} = -\dot{q} \quad (29)$$

where $J = -\Phi_q^{-1}\Phi_x$

5.1 Singularity Searching Method

A GA-based approach proposed to search singular points over the available workspace is addressed. For this method to operate, we first partition the workspace into several tiny zones.

Coding and decoding: GAs work with a population of chromosomes or strings. In the proposed GA, the strings for the coordinate parameters expanded by $(x, y, z, \phi, \theta, \psi)$ are formed by concatenating sub-strings, each of which is a binary coding of a parameter of the search space expressed by

$$s_r = s_{r1}s_{r2}s_{r3}s_{r4}s_{r5}s_{r6} \quad (30)$$

Using the binary coding method, every element, θ_k , of the parameter vector $\theta = [x \ y \ z \ \phi \ \theta \ \psi]^T$ is coded as a string of l_k for the desired resolution R_k :

$$R_k = \frac{\theta_{kh} - \theta_{kl}}{2^{l_k} - 1}$$

A set S of individuals, called a population, is expressed as:

$$S = \{s_1, s_2, \dots, s_m\}$$

The decoding process is simply an inverse procedure of the coding process.

Cost function: The fitness evaluation function is a measure to evaluate the suitability of a chromosome. An appropriate cost function is defined by

$$\mathfrak{J} = |\det[J(x, y, z, \phi, \theta, \psi)]| \quad (31)$$

Reproduction: The chromosome of the current reproduction in each generation is reproduced in the next generation according to the reproduction probability

$$p_n = \frac{F_{si}}{\sum_{i=1}^{p_i} F_{si}}$$

Crossover: Two chromosomes in the mating pool are first selected randomly according to the crossover probability p_c and their information are interchanged.

Mutation: Randomly alternate a bit in the string, which assists in keeping delivery in the population. It is used to ensure that all points in the search space can be ultimately researched according to the mutation probability p_m .

6. PATH PLANNING AND SINGULARITY AVOIDANCE

Assume that the initial positions of the object and goal are specified. Furthermore, we characterize a minimal cuboid, with the width $\bar{x} - \underline{x}$, the length $\bar{y} - \underline{y}$, and the height $\bar{z} - \underline{z}$, that can include the whole workspace inside it. The whole 3D workspace is then partitioned into l equal slices each part equally portioned into $m \times n$ regions in 2D space. This yields the range of each sub-cuboid, with origin $(x_{ijk}, y_{ijk}, z_{ijk})$, characterized by

$$Z_{ijk} \equiv \left\{ \left[x_{ijk}, x_{ijk} + \delta x_{ijk} \right], \left[y_{ijk}, y_{ijk} + \delta y_{ijk} \right], \left[z_{ijk}, z_{ijk} + \delta z_{ijk} \right] \right\},$$

$$i = 1, \dots, l, j = 1, \dots, m, k = 1, \dots, n$$

where $\delta x_{ijk} = \frac{\bar{x} - \underline{x}}{m}$, $\delta y_{ijk} = \frac{\bar{y} - \underline{y}}{n}$, $\delta z_{ijk} = \frac{\bar{z} - \underline{z}}{l}$.

Fitness: Suppose that w is the number of singular areas existing on the i -th slice of the workspace, an appropriate fitness function is proposed as

$$F_p(x, y, z) = \sum_{i=1}^l \left[\alpha \frac{1}{l_i} + \beta \sum_{j=1}^w d_{ij} \prod_{j=1}^w P_{d_{ij}} \right] \quad (32)$$

with

$$P_{d_{ij}} = \begin{cases} 1, & \text{if } d_{ij} \geq 2r \\ 0, & \text{otherwise} \end{cases}$$

where α and β are the weighting factors, which can be used to shape the path profile for the moving platform; and

$$l_i = \frac{|p_i \bar{g} \times s \bar{g}|}{|s \bar{g}|} + \mathcal{E}$$

\mathcal{E} is a small positive constant, and

$$d_{ij} = \frac{|o_j p_i \times s p_i|}{|s p_i|}$$

7. DNA COMPUTING ALGORITHM

The concept of DNA computing algorithm uses chromosomes of DNA to illustrate specific optimization problems. The basic elements of biological DNA are nucleotides. Due to their different chemical structure, nucleotides can be

classified as four bases: Adenine (A), Guanine (G), Cytosine (C) and Thymine (T).

Coding and decoding: To tackle the path planning problem, the initial DNA sequences are generated randomly. Each sequence is divided into n parts and every part is corresponding to a slice. Each slice on the search space is further partitioned in to $m \times n$ regions. The DNA sequence is firstly decoded by the complementary relationship of DNA nucleotides. In this decoding scheme the relationship between the DNA molecules is defined by $A=\bar{T}$, $T=\bar{A}$, $C=\bar{G}$, $G=\bar{C}$.

Crossover: Crossover is a process of exchanging genetic information between two DNA sequences. For simplicity, the one-point crossover is adopted where the crossover point is assigned uniformly at random.

Mutation: The mutation of DNA algorithm is quite different from GAs in which the randomly selected bit is replaced by its complement. For DNA algorithms, the randomly selected bit in the sequence is replaced by the rule that ‘‘A’’ changes to ‘‘T’’, ‘‘C’’ changes to ‘‘G’’, and vice versa.

Virus and Enzyme: The enzyme operator refers to deletion, in which one or more base pairs are removed whereas the virus operator refers to insertion where one or more base pairs are inserted into sequence. They can be used to expand or shrink chromosome sequences. See Figs. 8 and 9.

The use of virus and enzyme operations is closed related to the distribution of singularities and the optimal path in workspace. In the original equally portioned slices on the search space, the distances (i.e. d_{or} and d_{op}) between the reference path, programmed path and areas of singularity are calculated respectively. Define $d_{ratio}^i = \frac{d_{or}^i}{d_{op}^i}$, see Fig

10. Furthermore, we define

$$d_{total_ratio} = \sum_{i=1}^m d_{ratio}^i, \quad d_{prob}^i = \frac{d_{ratio}^i}{d_{total_ratio}}, \quad i=1, \dots, m$$

The roulette wheel selection technique is applied with reference to d_{prob}^i to determine whether an enzyme or a virus operation ought to be executed on each originally equally portioned slice. For a slice with a large d_{prob}^i , the virus operation is suggested which means that the obstacles may be close to the programmed path.

7. DEMONSTRATION AND VERIFICATION

Singularities of the 3-legs 6 degree-of-freedom platform distributed on six areas have been obtained previously. Suppose that coordinates of the known start and goal points were respectively given by $[-131.25 \ -118.125 \ 998.125]$ (mm) and $[131.25 \ 118.125 \ 1251.875]$ (mm). The optimal moving path was obtained by applying the proposed

evolutionary method with the fitness function defined by (32) and the weighting factors α and β being 1 and 0.01, respectively. The specific path planning was found after 1000 generations. Figure 11 shows the resulting path generation. From the path planning figures we found that the paths obtained were not smooth enough (the best solution should be close to the reference path while avoiding the singular zones) due to genetic drift.

Suppose that coordinates of the known start and goal points were respectively given by $[-112.5 \ -101.25 \ 1016.25]$ (mm) and $[150. \ 135. \ 1270.]$ (mm). After specifying the singular region and start and goal positions, the genetic searching algorithm is activated in the path planner to generate via-points for a short and safe path to the goal.

6. CONCLUSIONS

This paper presents modeling, singularity characterization and optimal path planning design for a prototype 3-legs 6-DOF parallel manipulator. The issues of characterizing kinematic and dynamic models, workspace, singularity and path planning of the platform are presented. A novel process for searching the manipulator’s singularity based on the DNA algorithm is developed. A DNA-based path planning scheme is also proposed for navigation of the moving platform over the workspace while avoiding singularities.

ACKNOWLEDGMENT

This research was sponsored by National Science Council, Taiwan, R.O.C. under the grant NSC 93-2212-E-005-005.

REFERENCES

- Adeleman, L. M. (1998). Computing with DNA. *Scientific American*, pp. 54-61,.
- Ceccarelli, M., (1997). A new 3 D.O.F. spatial parallel mechanism. *Mechanism and Machine Theory*, **32**, pp. 895-902.
- Ding, Y. and Ren R. (2000). DNA genetic algorithm for design of the generalized membership-type Takagi-Sugeno fuzzy control system. *Proc. of IEEE International Conference on Systems, Man, and Cybernetics*, pp. 3862-3867.
- Fichter, E. F. (1986). A Stewart platform-based manipulator general theory and practical construction. *International Journal of Robotics Research*, **5(2)**, pp. 157-182.
- Garzon, M. H. and Deaton, R. J. (1999). Bimolecular computing and programming. *IEEE Transactions on Evolutionary Computation*, **3**, pp. 236-250,.
- Honegger, M., Codourey, A., and Burdet, E., 1997, ‘‘Adaptive control of the Hexaglide, a 6 dof parallel manipulator,’’ *Proceedings of IEEE International Conference on Robotics and Automation*, pp. 543-548.
- Kiguchi, K., Watanabe, K. and Fukuda, T. (2001). Trajectory planning of mobile robots using DNA

computing. *Proc. Of IEEE International Symposium on Computational Intelligence in Robotics and Automation*, pp. 380-385.

Madhav, S., (1989). *Quality Engineering Using Robust Design*. AT&T Bell Laboratories.

Raghavan, M. (1993). The Stewart platform of general geometry has 40 configurations. *ASME Journal of Mechanical Design*, **115(2)**, pp. 277-282.

Ryu, J. H., Song, J., and Kwon, D. S. (2001). A nonlinear friction compensation method using adaptive control and its practical application to an in-parallel actuated 6-DOF manipulator. *Control Engineering Practice*, **9**, pp. 159-167.

Stewart, D. (1965). A platform with six degrees-of-freedom. *Proceedings of Institution of Mechanical Engineers*, **180(Pt 1, 5)**, pp. 371-386.

Wang, J., and Gosselin, C. (1997). Kinematic analysis and singularity representation of spatial five-degree-of-freedom parallel mechanism. *Journal of Robotic Systems*, **14(2)**, pp. 851-869.



Fig. 1 The experimental parallel manipulator

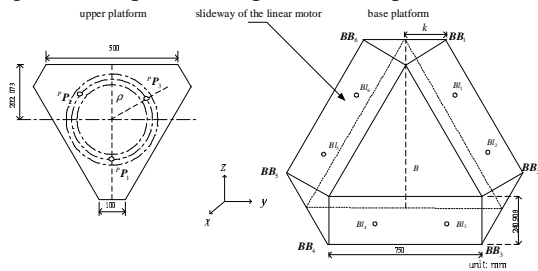


Fig. 2 Top view of the upper and base platforms

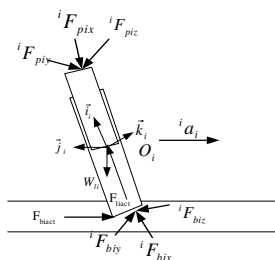


Fig. 3 Force and torque of the linear motor and link

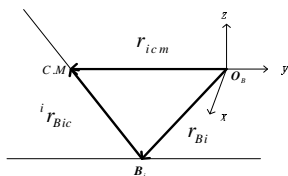


Fig. 4 Relation between link and joint of the linear motor

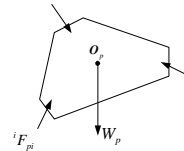


Fig. 5 Force and torque on the upper platform

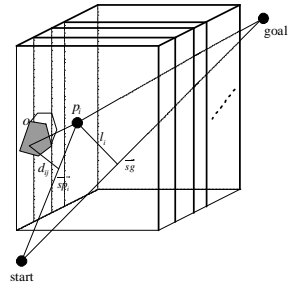


Fig. 6 Path computation in 3D space

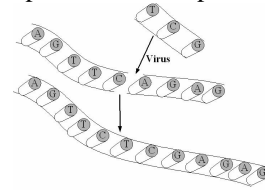


Fig. 8 Virus operation

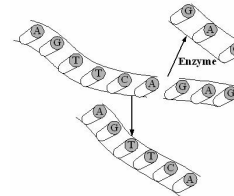


Fig. 9 Enzyme operation

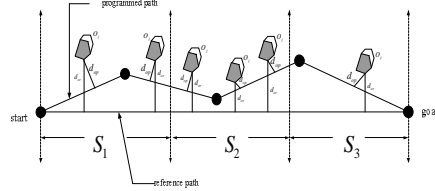


Fig. 10 Definitions of d_{or} and d_{op}

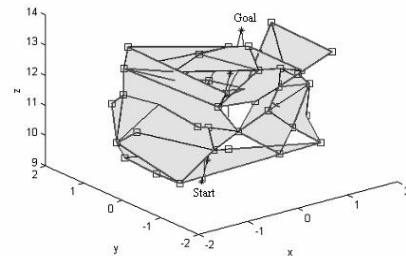


Fig. 11 Path generation-I while avoiding the whole singular area (unit: 100 mm)